Applied Physics Letters

Metal/$BaTiO_3$/β-Ga_2O_3 dielectric heterojunction diode with 5.7 MV/cm breakdown field

Cite as: Appl. Phys. Lett. **115**, 252104 (2019); https://doi.org/10.1063/1.5130669
Submitted: 06 October 2019 . Accepted: 04 December 2019 . Published Online: 17 December 2019

Zhanbo Xia, Hareesh Chandrasekar, Wyatt Moore, Caiyu Wang, Aidan J. Lee, Joe McGlone, Nidhin Kurian Kalarickal, Aaron Arehart, Steven Ringel, Fengyuan Yang, and Siddharth Rajan

Applied Physics Letters ARTICLE scitation.org/journal/apl

Metal/$BaTiO_3$/β-Ga_2O_3 dielectric heterojunction diode with 5.7 MV/cm breakdown field

Cite as: Appl. Phys. Lett. **115**, 252104 (2019); doi: 10.1063/1.5130669
Submitted: 6 October 2019 · Accepted: 4 December 2019 ·
Published Online: 17 December 2019

Zhanbo Xia,[1,a)] Hareesh Chandrasekar,[1] Wyatt Moore,[1] Caiyu Wang,[1] Aidan J. Lee,[3] Joe McGlone,[1] Nidhin Kurian Kalarickal,[1] Aaron Arehart,[1] Steven Ringel,[1,2] Fengyuan Yang,[3] and Siddharth Rajan[1,2,a)]

AFFILIATIONS

[1]Electrical & Computer Engineering, The Ohio State University, Columbus, Ohio 43210, USA
[2]Materials Science and Engineering, The Ohio State University, Columbus, Ohio 43210, USA
[3]Department of Physics, The Ohio State University, Columbus, Ohio 43210, USA

[a)]**Authors to whom correspondence should be addressed**: xia.104@osu.edu and rajan.21@osu.edu

ABSTRACT

Wide and ultrawide bandgap semiconductors can provide excellent performance due to their high energy bandgap, which leads to breakdown electric fields that are more than an order of magnitude higher than conventional silicon electronics. In materials where p-type doping is not available, achieving this high breakdown field in a vertical diode or transistor is very challenging. We propose and demonstrate the use of dielectric heterojunctions that use extreme permittivity materials to achieve a high breakdown field in a unipolar device. We demonstrate the integration of a high permittivity material $BaTiO_3$ with n-type β-Ga_2O_3 to enable a 5.7 MV/cm average electric field and a 7 MV/cm peak electric field at the device edge while maintaining forward conduction with relatively low on-resistance and voltage loss. The proposed dielectric heterojunction could enable improved design strategies to achieve theoretical device performance limits in wide and ultrawide bandgap semiconductors where bipolar doping is challenging.

The potential of different materials for vertical power switching is often assessed by calculating the Baliga Figure of Merit $\frac{V_{BR}^2}{R_{ON}} = \frac{\mu\epsilon E_c^3}{8}$.[1] In the case of wide and ultrawide bandgap materials, the high breakdown fields and the relatively good transport properties make the Baliga Figure of Merit significantly higher than conventional Si electronics. However, the breakdown field predicted for a material is based on a rectifying junction with the barrier height that is the same as the material bandgap energy, such as the PN junction. This is challenging to achieve in several wideband gap materials where bipolar doping is not available or presents technological challenges. Schottky junctions can provide excellent rectification, but the reverse breakdown of Schottky rectifiers is limited by the Schottky barrier height, which is significantly lower than the bandgap in most wideband gap semiconductors.[2–4] In this work, we show, using the case of β-Ga_2O_3, a dielectric heterojunction approach that can enable field management so that high breakdown fields can be achieved even in unipolar junctions.

The large breakdown electric field (6–8 MV/cm)[5] and electron mobility (250–300 $cm^2/V\,s$)[6] provide β-Ga_2O_3 a higher figure of merit than SiC and GaN. The availability of large area, high-quality bulk substrates from melt-growth methods[7–10] also provides a significant advantage for low-cost high-power devices. High voltage β-Ga_2O_3 transistors[11–15] and Schottky barrier diodes[16–19] with various designs have been reported in recent years. However, due to high acceptor activation energy and poor hole transport properties, p-type β-Ga_2O_3 is challenging to use in devices. The maximum effective breakdown field in vertical β-Ga_2O_3 devices is therefore limited by the Schottky barrier height to below 3.5 MV/cm. The breakdown of the β-Ga_2O_3 MOS structure with dielectrics (SiO_2, Al_2O_3, and HfO_2) is also limited by the metal/dielectric barrier height and is seen to occur far below the material breakdown limit of β-Ga_2O_3.

We now discuss the design principle of a dielectric heterojunction diode. The schematics and simulated energy band diagram of the dielectric heterojunction diode are shown in Figs. 1(a)–1(c). It consists of a 20 nm high-k $BaTiO_3$ layer ($\varepsilon_r \sim 260$) on a β-Ga_2O_3 lightly doped n-type drift layer. A Schottky metal contact is formed on the $BaTiO_3$ layer. $BaTiO_3$ is a perovskite material with a bandgap of 3.4 eV. It has an electron affinity of 3.8 eV,[20] which is close to the value of β-Ga_2O_3. Thus, the conduction band offset between $BaTiO_3$ and β-Ga_2O_3 is expected to be low. The Schottky barrier diode with the same β-Ga_2O_3 drift layer was also simulated as a comparison [Figs. 1(d)–1(f)].

Under reverse bias, the conduction band of the Schottky barrier diode inclines sharply due to the electric field, resulting in a thin triangular electron barrier. As a result, β-Ga_2O_3 Schottky barrier diodes

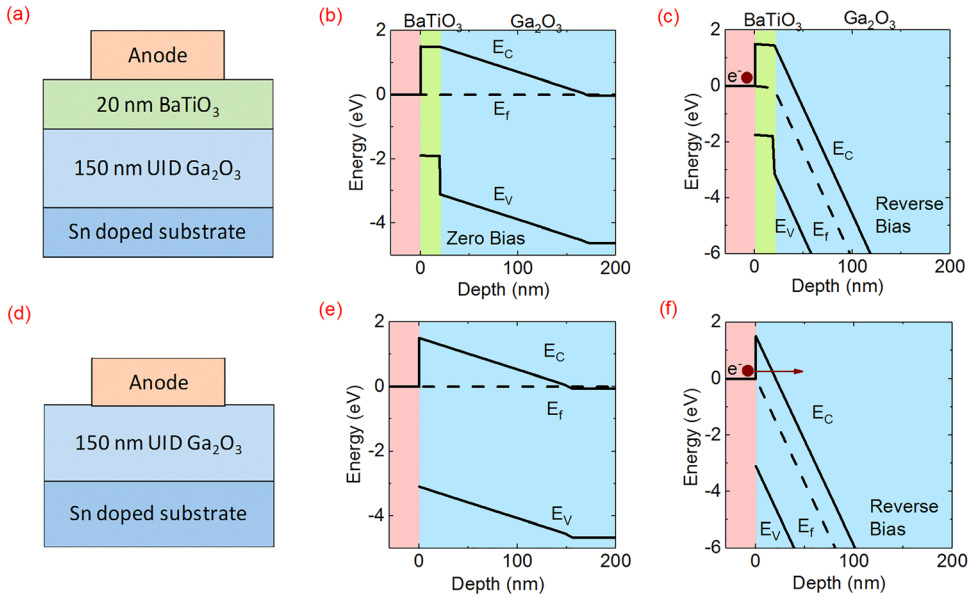

FIG. 1. (a) Schematics, (b) zero-biased band diagram, and (c) reverse bias band diagram of the $BaTiO_3/\beta$-Ga_2O_3 dielectric heterojunction. (d) Schematics, (e) zero-biased band diagram, and (f) reverse bias band diagram of the β-Ga_2O_3 Schottky barrier diode.

show tunneling breakdown at relatively low peak fields (typically ~3 MV/cm) due to Fowler-Nordheim tunneling. When the $BaTiO_3/\beta$-Ga_2O_3 dielectric heterojunction diode is reverse-biased, the electric field in the β-Ga_2O_3 drift layer is similar to the Schottky diode in the previous case. However, due to the large dielectric constant discontinuity between $BaTiO_3$ and β-Ga_2O_3, the electric field in $BaTiO_3$ is lower by a factor $\frac{\epsilon_{BTO}}{\epsilon_{GOX}}$ ($\sim$ 26 in this case) of the value in β-Ga_2O_3. As a result, the conduction band profile in $BaTiO_3$ remains flat, blocking the electrons tunneling from metal to β-Ga_2O_3 under higher reverse bias. Therefore, the $BaTiO_3/\beta$-Ga_2O_3 dielectric heterojunction maintains an effective potential barrier at much higher voltages than the metal/semiconductor junction.

Under forward bias, electrons must flow from the semiconductor, through the high dielectric constant layer, into the metal. For a small value of the conduction band offset between $BaTiO_3/\beta$-Ga_2O_3 (as predicted from the electron affinity difference), the dielectric heterojunction will have a small effective barrier to transport. Since $BaTiO_3$ is an insulator, the injected current is expected to be limited by space-charge limited transport, which has a dependence $J \sim \frac{\mu\epsilon V^2}{L^3}$, where μ is the electron mobility, ϵ is the dielectric constant, and L is the thickness of the dielectric. Therefore, while the mobility of carriers in $BaTiO_3$ may be low, the high dielectric constant will help to decrease the voltage drop in the dielectric. Therefore, the $BaTiO_3/\beta$-Ga_2O_3 dielectric heterojunctions are expected to be turned on under forward bias.

To characterize the breakdown field of the dielectric heterojunction without additional field termination processes, we fabricated Schottky diodes and $BaTiO_3/\beta$-Ga_2O_3 diodes on relatively thin drift regions consisting of 150 nm unintentional doped (UID) β-Ga_2O_3 on an n-type substrate. The UID β-Ga_2O_3 drift layer was grown by oxygen plasma-assisted molecular beam epitaxy (MBE), using growth conditions reported earlier.[21] To prevent further electron depletion into the substrate at high reverse bias, a 10 nm heavily doped n-type ($\sim 5 \times 10^{19}$ cm^{-3}) β-Ga_2O_3 layer was grown before the 150 nm UID layer. The electron concentration in UID β-Ga_2O_3 was estimated from capacitance-voltage profiling to be lower than 10^{16} cm^{-3}. A 20 nm $BaTiO_3$ layer was deposited on β-Ga_2O_3 by physical vapor deposition in Ar/O_2 ambience with a flow rate of 20:2 sccm. A plasma power of 140 W and a chamber pressure of 10 mTorr were maintained during deposition. A deposition rate of 0.5 nm/min was confirmed by ellipsometry. A dielectric constant of 260 ± 20 was measured from C-V measurements (the details are discussed in the supplementary material). A metal stack of Pt/Au (30 nm/100 nm) was deposited by an electron beam evaporator to form square Schottky contact pads (50 μm $\times$ 50 μm) on both the β-Ga_2O_3 sample and the $BaTiO_3/\beta$-Ga_2O_3 sample. 30 nm Ti followed by 100 nm Au was deposited on the backside of the n-type substrate to form Ohmic contacts.

The β-Ga_2O_3 UID layer thickness of 150 ± 3 nm was confirmed by the C-V measurement on the Schottky junction diodes. Reverse bias measurements of 10 dielectric heterojunctions and 10 Schottky diodes were performed. The breakdown voltage was taken as that required to induce a current density of 1 A/cm^2. The resulting breakdown voltages for the two types of devices are summarized in Fig. 2(a). The mean breakdown voltage was 83.3 V for the dielectric heterojunctions and 44.5 V for the Schottky junctions. The characteristic I-V curves of devices with near-mean behavior are shown in Fig. 2(b). The Schottky barrier diode had a breakdown voltage of 45 V, which corresponds to a breakdown field of 3 MV/cm. This breakdown field is comparable with previous reports.[14,15] The $BaTiO_3/\beta$-Ga_2O_3 heterojunction diode showed a significantly higher breakdown voltage of 85 V, corresponding to a peak electric field of 5.7 MV/cm (calculated assuming background doping $= 10^{16}$ cm^{-3} and a 150 nm depletion width). This is the highest breakdown electric field reported for a vertical β-Ga_2O_3 device. The 2D electric field profile of the dielectric heterojunction at the breakdown scenario was simulated using Sivalco ATLAS[22]

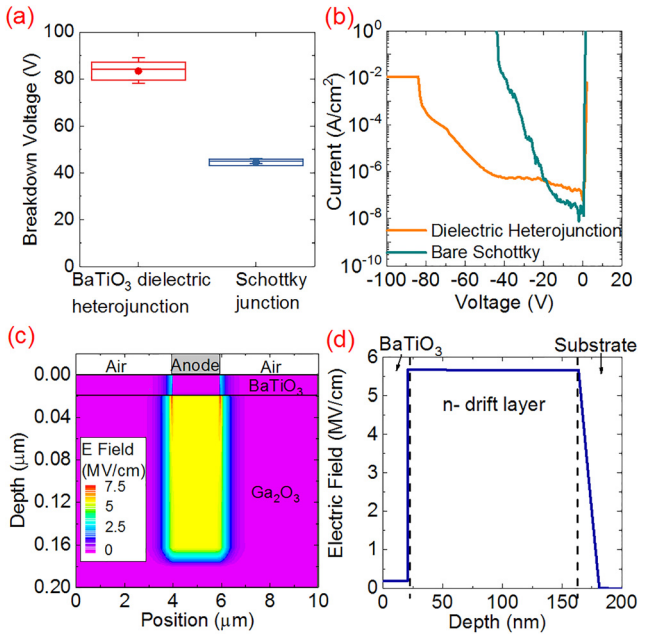

FIG. 2. (a) Statistical summary of the measured breakdown voltage of 10 devices from the dielectric heterojunctions and the Schottky junctions. (b) I-V characteristics under reverse bias (c) simulated 2D electric field profile of the dielectric heterojunction at breakdown bias (note the difference between x and y dimensions). (d) Simulated electric field profile of the dielectric heterojunction from the metal/$BaTiO_3$ interface to the n+ substrate.

[Figs. 2(b) and 2(c)]. It can be seen from the simulation that when the electric field at the center of the device is 5.7 MV/cm, the edge of the device is expected to have an electric field of 7 MV/cm.

We now discuss the breakdown mechanism of the $BaTiO_3$/β-Ga_2O_3 dielectric heterojunction. The Poole-Frenkel plot of the dielectric heterojunction [Fig. 3(a)] under reverse bias (40 V–70 V) shows near-linear behavior, suggesting that the breakdown mechanism is governed by trap-assisted tunneling (Poole-Frenkel emission).[23] The corresponding traps could be located in either the $BaTiO_3$ region or the β-Ga_2O_3 region. The temperature dependent currents under reverse bias were measured, and the Arrhenius plot with respect to the field in $BaTiO_3$ is plotted in Fig. 3(b). A trap energy level of 0.25 eV was extracted from the slope, assuming that the corresponding traps are located in the $BaTiO_3$ layer. The same temperature dependent data were fit, assuming an Arrhenius dependence on the electric field in β-Ga_2O_3 [Fig. 3(c)]. This fit suggests a trap energy of 0.6 eV if the traps are in β-Ga_2O_3. The electric field used in this calculation was estimated in the center region of the device. However, the edges of the device have a much higher electric field under reverse bias, and they are likely to be the regions where breakdown occurred. Therefore, the extracted trap energy level may be suggestive but not entirely accurate. Further experiments and studies are needed to confirm the location and energy of the corresponding traps. Our current results show that the breakdown voltage of the dielectric heterojunction is not fundamentally limited by the band structure, suggesting that improvement in the quality of $BaTiO_3$ and β-Ga_2O_3 may further increase the breakdown field of the dielectric heterojunction.

Under forward bias, the Schottky junction and dielectric heterojunction showed on-resistances of 1.4 mΩ cm^2 and 1.5 mΩ cm^2, respectively [Fig. 4(a)]. The 20 nm $BaTiO_3$ layer added a 0.1 mΩ cm^2 extra on-resistance once the device is turned on. The turn-on voltage was 1.5 V for the Schottky diode and 3.5 V for the dielectric heterojunction diode. The voltage drop across the $BaTiO_3$/β-Ga_2O_3 junction could be due to a band offset or due to a resistive drop across the $BaTiO_3$. To investigate the mechanism, we plotted the IV characteristics on a Fowler-Nordheim[24] plot. The linear fit on the Fowler-Nordheim plot [Fig. 4(b)] suggests that the transport is limited by a tunneling mechanism across a triangular barrier. Assuming that the barrier was due to the conduction band offset, the characteristic barrier height was estimated to be 0.08 eV [Fig. 4(c)]. Therefore, it seems likely that the transport is indeed limited by the conduction band barrier between $BaTiO_3$ and β-Ga_2O_3.

In conclusion, we have proposed and demonstrated the concept of dielectric heterojunctions that use extreme permittivity materials to achieve a high breakdown field in a unipolar device. We showed a $BaTiO_3$/β-Ga_2O_3 dielectric heterojunction diode with the record-high electric field of 5.7 MV/cm measured in β-Ga_2O_3. The dielectric heterojunction shows a turn-on voltage of 3.5 V and an on-resistance of 1.5 mΩ cm^2. This structure demonstrated here not only brings up a design for the high performance β-Ga_2O_3 diode but also can be used as a gate dielectric barrier in both lateral and vertical transistors. This dielectric heterojunction concept can also be expanded to other semiconductor materials in which the bipolar device is technically challenging, such as SiC, GaN, ZnO, and diamond. It may also be useful to Si and III-V

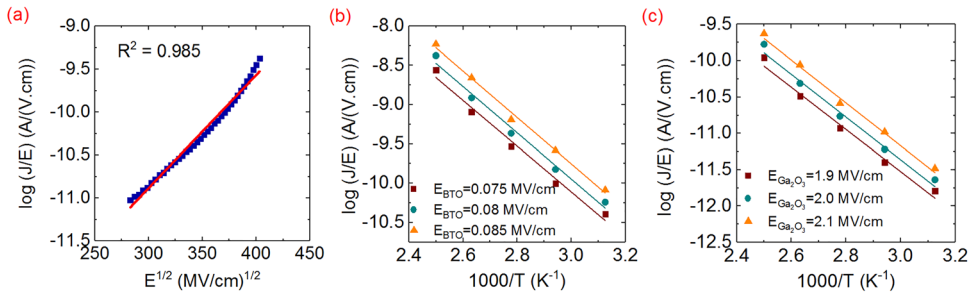

FIG. 3. (a) The Poole-Frenkel plot of the dielectric heterojunction under reverse bias (40 V-70 V) and the Arrhenius plot measured from 300 K to 400 K using the electric field in (b) $BaTiO_3$ and (c) β-Ga_2O_3.

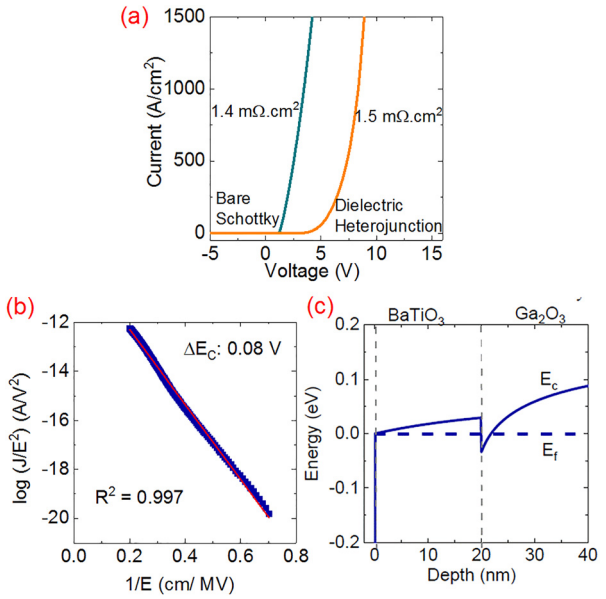

FIG. 4. (a) On-state characteristics of the dielectric heterojunction diode and Schottky diode. (b) The Fowler-Nordheim tunneling plot of the dielectric heterojunction diode under the forward bias condition. (c) Simulated conduction band diagram of the dielectric heterojunction under the forward bias condition (+1.5 V).

materials to achieve a faster unipolar device with higher breakdown voltage than typical Schottky barrier diodes.

See the supplementary material for details about the measurement of the $BaTiO_3$ dielectric constant.

This work was funded by the National Science Foundation ECCS-1809682 and AFOSR GAME MURI (Grant No. FA9550-18-1-0479, Program Manager Dr. Ali Sayir). Aidan J. Lee and Fengyuan Yang acknowledge the support by the Center for Emergent Materials, an NSF MRSEC (Grant No. DMR-1420451).

REFERENCES

[1]B. J. Baliga, J. Appl. Phys. **53**, 1759 (1982).
[2]A. Itoh, T. Kimoto, and H. Matsunami, IEEE Electron Device Lett. **16**(6), 280–282 (1995).
[3]L. Wang, M. I. Nathan, T.-H. Lim, M. A. Khan, and Q. Chen, Appl. Phys. Lett. **68**(9), 1267 (1996).
[4]E. Farzana, Z. Zhang, P. K. Paul, A. R. Arehart, and S. A. Ringe, Appl. Phys. Lett. **110**, 202102 (2017).
[5]M. Higashiwaki, K. Sasaki, A. Kuramata, T. Masui, and S. Yamakoshi, Appl. Phys. Lett. **100**, 013504 (2012).
[6]N. Ma, N. Tanen, A. Verma, Z. Guo, T. Luo, H. Xing, and D. Jena, Appl. Phys. Lett. **109**(21), 212101 (2016).
[7]Z. Galazka, R. Uecker, K. Irmscher, M. Albrecht, D. Klimm, M. Pietsch, M. Brützam, R. Bertram, S. Ganschow, and R. Fornari, Cryst. Res. Technol. **45**, 1229 (2010).
[8]H. Aida, K. Nishiguchi, H. Takeda, N. Aota, K. Sunakawa, and Y. Yaguchi, J. Appl. Phys. **47**, 8506 (2008).
[9]S. Ohira, N. Suzuki, H. Minami, K. Takahashi, T. Araki, and Y. Nanishi, Phys. Status Solidi C **4**, 2306 (2007).
[10]E. G. Víllora, K. Shimamura, Y. Yoshikawa, K. Aoki, and N. Ichinose, J. Cryst. Growth **270**(3–4), 420–426 (2004).
[11]M. H. Wong, K. Sasaki, A. Kuramata, S. Yamakoshi, and M. Higashiwaki, IEEE Electron Device Lett. **37**(2), 212–215 (2016).
[12]A. J. Green, K. D. Chabak, E. R. Heller, R. C. Fitch, M. Baldini, A. Fiedler, K. Irmscher, G. Wagner, Z. Galazka, S. E. Tetlak *et al.*, IEEE Electron Device Lett. **37**(7), 902–905 (2016).
[13]Z. Hu, K. Nomoto, W. Li, N. Tanen, K. Sasaki, A. Kuramata, T. Nakamura, D. Jena, and H. G. Xing, IEEE Electron Device Lett. **39**(6), 869–872 (2018).
[14]C. Joishi, Y. Zhang, Z. Xia, W. Sun, A. R. Arehart, S. Ringel, S. Lodha, and S. Rajan, IEEE Electron Device Lett. **40**(8), 1241–1244 (2019).
[15]K. Zeng, A. Vaidya, and U. Singisetti, "1.85 kV Breakdown voltage in lateral field-plated Ga_2O_3 MOSFETs," IEEE Electron Device Lett. **39**(9), 1385–1388 (2018).
[16]W. Li, Z. Hu, K. Nomoto, R. Jinno, Z. Zhang, T. Q. Tu, K. Sasaki, A. Kuramata, D. Jena, and H. G. Xing, *IEEE International Electron Devices Meeting (IEDM)* (IEEE, 2018), pp. 8–5.
[17]K. Konishi, K. Goto, H. Murakami, Y. Kumagai, A. Kuramata, S. Yamakoshi, and M. Higashiwaki, Appl. Phys. Lett. **110**(10), 103506 (2017).
[18]K. Sasaki, D. Wakimoto, Q. T. Thieu, Y. Koishikawa, A. Kuramata, M. Higashiwaki, and S. Yamakoshi, IEEE Electron Device Lett. **38**(6), 783–785 (2017).
[19]J. Yang, S. Ahn, F. Ren, S. J. Pearton, S. Jang, and A. Kuramata, IEEE Electron Device Lett. **38**(7), 906–909 (2017).
[20]F. M. Michel-Calendini and G. Mesnard, J. Phys. C **6**, 1709 (1973).
[21]S. Krishnamoorthy, Z. Xia, S. Bajaj, M. Brenner, and S. Rajan, Appl. Phys. Express **10**(5), 051102 (2017).
[22]See https://www.silvaco.com/products/tcad/device_simulation/atlas/atlas.html for information about SILVACO ATLAS.
[23]J. Frenkel, Phys. Rev. **54**(8), 647 (1938).
[24]R. H. Fowler and L. Nordheim, "Electron emission in intense electric fields," Proc. R. Soc. London, Ser. A **119**(781), 173–181 (1928).